

Video Article

Use of Real-Time Functional Magnetic Resonance Imaging-Based Neurofeedback to Downregulate Insular Cortex in Nicotine-Addicted Smokers

Mohit Rana^{1,2,3}, Sergio Ruiz^{1,2}, Andrea Sánchez Corzo^{1,2}, Axel Muehleck⁴, Sandra Eck⁴, César Salinas⁴, Francisco Zamorano^{4,5}, Claudio Silva⁴, Massimiliano Rea⁴, Anil Batra⁴, Niels Birbaumer^{1,7,8}, Ranganatha Sitaram^{1,2,9}

¹Departamento de Psiquiatría, Escuela de Medicina, Centro Interdisciplinario de Neurociencias, Pontificia Universidad Católica de Chile

²Laboratory for Brain-Machine Interfaces and Neuromodulation, Pontificia Universidad Católica de Chile

³Institute of Medical Psychology and Behavioral Neurobiology, University of Tübingen

⁴Department of Psychiatry and Psychotherapy, University of Tübingen

⁵Unidad de Imágenes Cuantitativas Avanzadas, Departamento de Imágenes, Facultad de Medicina, Clínica Alemana de Santiago

⁶División de Neurociencia, Centro de Investigación en Complejidad Social (neuroCICS), Facultad de Gobierno, Universidad del Desarrollo

⁷Institute di Ricovero e Cura a Carattere Scientifico

⁸Wyss Center for Bio and Neuroengineering

⁹Institute for Biological and Medical Engineering, Pontificia Universidad Católica de Chile

Correspondence to: Mohit Rana at morana@uc.cl, Sergio Ruiz at sruiz@uc.cl, Ranganatha Sitaram at rasitaram@uc.cl

URL: <https://www.jove.com/video/59441>

DOI: [doi:10.3791/59441](https://doi.org/10.3791/59441)

Keywords: nicotine dependence, real-time fMRI, insula, addiction, neurofeedback, smoking cessation, cue-induced craving

Date Published: 5/19/2020

Citation: Rana, M., Ruiz, S., Corzo, A.S., Muehleck, A., Eck, S., Salinas, C., Zamorano, F., Silva, C., Rea, M., Batra, A., Birbaumer, N., Sitaram, R. Use of Real-Time Functional Magnetic Resonance Imaging-Based Neurofeedback to Downregulate Insular Cortex in Nicotine-Addicted Smokers. *J. Vis. Exp.* (), e59441, doi:10.3791/59441 (2020).

Abstract

It has been more than a decade since the first functional magnetic resonance imaging (fMRI)-based neurofeedback approach was successfully implemented. Since then, various studies have demonstrated that participants can learn to voluntarily control a circumscribed brain region. Consequently, real-time fMRI (rtfMRI) provided a novel opportunity to study modifications of behavior due to manipulation of brain activity. Hence, reports of rtfMRI applications to train self-regulation of brain activity and the concomitant modifications in behavioral and clinical conditions such as neurological and psychiatric disorders [e.g., schizophrenia, obsessive compulsive Disorder (OCD), stroke] have rapidly increased.

Neuroimaging studies in addiction research have shown that the anterior cingulate cortex, orbitofrontal cortex, and insular cortex are activated during the presentation of drug-associated cues. Also, activity in both left and right insular cortices have been shown to be highly correlated with drug urges when participants are exposed to craving-eliciting cues. Hence, the bilateral insula is of particular importance in researching drug urges and addiction due to its role in the representation of bodily (interoceptive) states. This study explores the use of rtfMRI neurofeedback for the reduction in blood oxygen-level dependent (BOLD) activity in bilateral insular cortices of nicotine-addicted participants. The study also tests if there are neurofeedback training-associated modifications in the implicit attitudes of participants towards nicotine-craving cues and explicit-craving behavior.

Introduction

Neurofeedback is an operant conditioning procedure through which humans or animals can learn to modulate neural activity in one or more brain regions. Training typically leads to behavioral modifications¹. In principle, brain signals from one or more circumscribed brain regions are transformed into sensory feedback (e.g., visual, auditory, or tactile feedback), which is provided to the participant for control of brain activity by operant conditioning or other forms of learning. In the reversal of the traditional neuroimaging paradigm, neurofeedback studies modulate brain activity as an independent variable and measure behavior as a dependent variable. Thus, neurofeedback provides a novel approach to investigating the involvement of brain regions in different cognitive functions and how hyper- or hypoactivation of those brain regions can lead to abnormal behavior.

Neurofeedback has been used with different neuroimaging modalities like functional magnetic resonance imaging (fMRI), electroencephalography (EEG), and functional near-infrared spectroscopy (fNIRS). EEG- and fNIRS-based neurofeedback paradigms have the advantages of higher temporal resolution, affordability, and portability^{2,3}. However, they are characterized by low spatial resolution and an inability to access deeper brain regions. In addition, EEG has the computational complexity of the inverse problem for determining a source of neural activations from surface EEG signals⁴. However, with recent developments in real-time fMRI (rtfMRI), it is possible to access hemodynamic signals from all parts of the brain, with good spatial resolution (e.g., 2 mm³) and a temporal resolution of 720 ms⁵. Thus, fMRI overcomes the above-mentioned limitations possessed by fNIRS and EEG techniques.

Addiction to nicotine is one of the major causes of death across the world due to a number of diseases associated with smoking⁶. Recognized factors leading to nicotine addiction are social, environmental, psychological⁷, and genetic susceptibility⁸. On a neurobiological level, studies have shown activation in the anterior cingulate cortex (ACC), orbitofrontal cortex (OFC), ventral tegmental area (VTA), ventral striatum,

amygdala, hippocampus, prefrontal cortex (PFC), and insular cortex during the presentation of drug-associated cues in contrast to neutral control cues^{9,10,11,12,13,14}. Activity in both left and right insulas are highly correlated with smoking urges when smokers viewed drug-associated cues^{15,16}. The insula plays an important role in eliciting craving behavior^{17,18,19,20,21}, as it is responsible for perception of the bodily state. It has been reported that smokers with lesions in their insular cortices were more likely to quit smoking than smokers with brain damage not involving the insula¹⁸.

One of the biggest challenges in existing smoking cessation methods is the high relapse rate²². More than 80% of smokers relapse within the first few months after quitting smoking²³. Exposure to cues previously associated with drug use is a major reason for the high relapse rate in nicotine addiction²⁴. This mechanism is called the incubation effect. The current protocol is developed to target the incubation effect assessed by an affective priming task. Previous studies have demonstrated that abstaining smokers have negative implicit attitudes toward smoking-related cues^{25,26,27,28}. In the typical affective priming task, emotional priming stimuli modify the processing of an affective target so that the reaction time and accuracy of responses are changed²⁹. In other words, if the prime and target stimuli are of the same valence, the reaction time in response to the target stimuli will be faster, and vice versa.

In the current study, it is hypothesized that downregulation of the bilateral anterior insular cortex will reduce craving, and hence, the valence of craving-inducing cues will change from negative to neutral, as attentional and associative biasing will move away from smoking-related cues³⁰. The implicit behavior task is an affective priming task originally adapted from Czyzewska and Graham³¹. Based on the aforementioned hypothesis, it is anticipated to observe a decrease in reaction time in response to a combination of prime (craving eliciting picture or its neutral counterpart picture) and target words with positive valence after downregulation block as compared to baseline block. The priming task (**Figure 2B**) consists of a prime (i.e., a craving eliciting picture or its neutral counterpart picture³²) and target word with positive or negative valence. The prime picture is presented for 200 ms, followed by a target word presented for 1 second. Stimulus onset asynchrony (SOA) is 250 ms. Participants are then instructed to judge the valence of the target word (positive or negative) and respond by pressing a button as quickly and accurately as possible.

The rtfMRI system (**Figure 1**) consists of the following subsystems: (1) participant, (2) signal acquisition, (3) online signal analysis, and (4) signal feedback. Signal acquisition is carried out with a 3.0T Siemens Trio whole-body scanner using an echo planar imaging (EPI) sequence³³. Procedures such as image reconstruction, distortion correction, and averaging of the signal are performed on the scanner computer. Once the images are reconstructed and preprocessed, they are exported to the signal analysis subsystem. The signal analysis subsystem is implemented using the Turbo Brain Voyager (TBV)³⁴. TBV retrieves the reconstructed images and performs data processing that includes 3D motion correction and real-time statistical analysis using the general linear model³⁵. TBV allows the user to draw regions of interest (ROIs) over multiple voxels on the functional images and extract average BOLD values of the ROI after each repetition time (TR). The time series of the selected ROIs are then exported to the MATLAB script that calculates and presents feedback to the participant.

Visual feedback of brain activity is provided to participants in the form of a graphically animated thermometer, with its bars changing in proportion to the percent BOLD changes in the ROIs. Several studies have used intermittent feedback (feedback provided to a participant after a number of TRs of the EPI sequence) for training participants^{36,37}. However, in the current study, it was anticipated that participants would have greater difficulty in downregulating the BOLD signal in the anterior insula with continuous feedback due to insula's role in sensory integration and involvement in processing visual feedback information³⁸. Hence, it was presumed that continuous feedback would result in a conflict between two processes in the insular cortex, one process that increases the signal due to external feedback, and another that decreases the signal due to neurofeedback training. Hence, in this study, we provide feedback only at the end of each downregulation block (delayed feedback). Participants are shown a text (e.g., Euro 0.87) as visual feedback (**Figure 2A,C**) that indicates the amount of money they earned (monetary reward). This reward is proportional to the percentage downregulation achieved in the regulation block.

RtfMRI is a novel neurotechnology that may be able to overcome problems in therapeutic approaches to addiction treatment and may provide more reliable and effective interventions for reducing relapse. The long-term objectives of the current study are three-fold: 1) to test whether nicotine addicts can learn to downregulate BOLD signals in the anterior insula during the presence of stimuli eliciting craving behavior; 2) to examine whether neurofeedback training leads to modifications in craving behavior; and 3) to explore whether changes in craving levels during neurofeedback training of downregulation of the insula persists after six months of training without any other intervention. This article provides a detailed description of the rtfMRI experimental protocol and its different components. Also presented are sample data from the study and a discussion of this method's future challenges and potential in addiction research. The protocol presented is designed to investigate whether fMRI-based neurofeedback training can be used to study reductions in brain activity in the insular cortex of cigarette smokers. In addition, the protocol is intended to study relationships between activation of the insular cortex and the craving behaviors of cigarette smokers.

Protocol

The Ethics Committee of the Medical Faculty of the University of Tübingen and Pontificia Universidad Católica de Chile approved the following rtfMRI protocol.

1. Hardware set-up

1. The hardware represented in **Figure 1** is prepared only once to set up the real-time export of the MRI data.
2. Preparation of the MRI room is the same as the traditional fMRI measurement. Prepare the MRI room before arrival of the participant.
3. Attach the 32 or 20 channels head coil to the scanner.
4. Connect the projector's VGA/HDMI cable and MR compatible response device (button box) to the stimulus computer.

NOTE: In most of the MR set-up, the response device delivers the TR-trigger to the stimulus computer. This trigger helps to synchronize stimulus presentation and data acquisition.

2. Participant preparation outside of the scanner

1. Prepare the consent form and questionnaires that participants need to fill out before their arrival.
2. Once the participant arrives, explain the experiment and fMRI technique. Also, instruct the participant on how to perform the task (e.g., during the experiment, participants must keep their eyes open and always look at the pictures on display screen, and they should try not to move their heads inside the scanner).
3. Ask the participant to sign the consent form and fill in the questionnaires required to assess craving levels.
4. Ask participants to fill out the following questionnaires: 1) VAS-C: Visual Analogue Scale, Craving³⁹, 2) QSU-b: Questionnaire of Smoking Urges–Brief Version⁴⁰, and 3) cigarettes per day.
5. Ask the participant to exhale through the carbon monoxide (CO) measuring device.
NOTE: CO measurement⁴¹ indicates whether or not the participant refrains from smoking at least 3 h before arrival for the neurofeedback session. CO is measured in ppm (parts per million). Low CO values indicate that the participant did not smoke for at least a couple of hours prior to arrival. Participants should be asked to refrain from smoking so that the craving cues elicit high craving during the experiment. Participants with high CO values will be cautioned prior to the future neurofeedback session to ensure that they refrain from smoking before the rfMRI session. Participants who do not refrain from smoking twice should be excluded from the study.

3. Participant positioning

NOTE: The procedure of participant positioning on the scanner table is similar to the traditional fMRI experiment.

1. Ask the participant to remove all metallic objects from his or her pockets before entering the MRI room.
2. Ask the participant to insert ear plugs before he or she lies down on the scanner table in a supine position.
3. Use pads to fix the head position of the participant inside the head coil. This step helps to reduce head movement during the measurement.
4. Lock the upper part of the head coil and fix the mirror to the head coil.
5. Give the response device to the participant and place the response device according to the comfort of the participant.
6. Ask the participant to close his or her eyes and mark the reference head position of the participant in between the eyebrows using laser light.
7. Move the scanner table to place the marked position to the center of the MRI bore.
8. Confirm with the participant that he or she is in comfortable position and that he or she can see the visual stimuli projected on the screen behind the scanner using the mirror. Adjust the mirror, if required.

4. Data acquisition

1. During the initial scans, ask the participant to close his or her eyes and try not to move the head.
2. Start the measurement with a localizer pulse sequence. This sequence is typically used to determine the slice position of the subsequently run anatomical scan and functional (EPI sequence) scans.
3. Select the field of view (FOV) for the anatomical scan with the following parameters: TR = 11.5 ms, TE = 5 ms, 176 slices without slice gap, FOV = 240 x 240mm², matrix = 256 x 256, flip angle = 18°, providing 1 mm³ isotropic voxels. The FOV of the sequence will cover the whole head of the participant.
4. The field of view for the functional (EPI sequence) scan is aligned to the anterior commissure/posterior commissure line (AC-PC line). Adjust the position of the slices to cover the target region of interest. The parameters of the sequence are the following: TR = 1.5, FOV = 192 mm, 25 slices, voxel = 3 mm x 3 mm x 3 mm, flip angle = 70°.

5. fMRI neurofeedback

1. Alert the participant that the neurofeedback run is starting and repeat the instructions provided earlier (e.g., that during the baseline, a block is represented by a "+" sign).
NOTE: The participant must observe the image on the display screen. On the other hand, during the regulation block, represented by an arrow in a downward direction, participants should try to detach themselves from craving urges using some cognitive strategies. The amount of money shown at the end of each regulation block represents their performance. A higher amount of money represents better performance.
2. Perform the neurofeedback run in which the baseline and regulation blocks are alternating (30 s each; **Figure 2**).
3. On the stimulus computer, run the stimulus code written presentation software and press the **Enter** button after **Ready** appears on the screen. Presentation code is now waiting for the trigger to start the neurofeedback run.
NOTE: The code is in sync with the TR triggers coming from the scanner. Therefore, it is the first step in preparation of running the neurofeedback run.
4. On the analysis computer, run the in-house MATLAB toolbox and turbo brain voyager (TBV).
5. In the MATLAB toolbox, enter the information specific to the participant, such as patient ID and neurofeedback run number.
6. Press **Generate protocol files** to prepare the protocol file using the information inserted in step 5.5.
NOTE: The protocol file contains information related to the condition timing (e.g., the time at which TR a specific condition should start and which stimulus to be presented). It will be used by both the MATLAB toolbox and TBV.
7. Press the button **execute** on the GUI of the MATLAB toolbox. The code is now waiting to receive data from the TBV.
8. In the TBV, select the protocol file generated in step 5.6. In addition, select the .roi file generated from the previous neurofeedback sessions.
NOTE: Selecting an ROI file is important, as it will avoid crashing of the TBV software during the initial (10 TRs) period of the neurofeedback run.
9. Prepare the EPI sequence to be implemented in the MR host computer. Press the start button in the TBV.
10. Redraw the target ROIs in the TBV software according to the anatomical landmarks. The shape and size of the ventricles in the brain are used as landmarks to select the anterior insula. In addition, the wavy shape of the insular cortex is used precisely select the voxels related to bilateral anterior insula.

11. Draw an ROI on the primary motor area (M1) using the central sulcus as an anatomical landmark. The primary motor area acts as a reference ROI to remove the effect of global BOLD increases and BOLD fluctuations due to head movement.
12. At the end of each neurofeedback session, ask the participant, "What cognitive strategy were you using during the regulation block?". In addition, ask the participant about his or her comfort level and whether or not she or she wishes to continue with the experiment.
13. After four neurofeedback runs, select the radio button **Yes** for the transfer run.
NOTE: A transfer run is similar to the neurofeedback run. However, participants perform self-regulation in absence of feedback. This helps to determine whether the learned self-regulation is transferred to the situation in which the participant will not receive neurofeedback (e.g., outside the scanner).

6. Control group

1. Instruct the participants in the control group in the same manner as those in the experimental group. However, provide yoked feedback to the participants.
NOTE: In yoked feedback, the average amount of reinforcement (money) in both the experimental and control groups remains the same. The only difference between the two groups is contingency of the feedback provided to participants. For participants in the control group, the total amount of reinforcement (money) is distributed among the randomly assigned 40% of the downregulation trials. However, in the other 60% of trials, participants receive negative feedback (zero Euros). Thus, the participants in the control group do not get contingent feedback.

7. Offline analysis

1. Preprocessing of fMRI data
 1. Use a statistical parametric mapping (SPM) toolbox to preprocess the fMRI data (<https://www.fil.ion.ucl.ac.uk/spm/ext/>).
 2. Convert the fMRI data in DICOM format to NIFTI format using format conversion utility of the SPM batch function.
 3. Remove the initial 10 scans from each neurofeedback run data to avoid gradient equilibration effects⁴².
 4. Perform the realignment process to remove motion artifacts and align all the volumes to the first volume of the session. In addition, perform time slice correction to compensate for the slice acquisition delay⁴³.
 5. Conduct segmentation of the anatomical scan, coregistration of the EPI sequence data and the anatomical data, and normalization to map the subject space data to the Montreal Neurological Institute (MNI) standard brain template⁴⁴.
 6. Using our in-house MATLAB code, extract the BOLD signals from cube-shaped ROIs created around the MNI coordinates corresponding to the bilateral anterior insula and primary motor cortex.
2. Calculation of percentage change in the BOLD signal
 1. Calculate the percentage change in the BOLD signal based on the average change in BOLD signal for each ROI during the regulation block compared to the previous baseline block. The equation for percentage change in the BOLD signal is the following:

$$\text{Percentage change} = \frac{\text{mean}(\text{BOLD}_{\text{regulation}}) - \text{mean}(\text{BOLD}_{\text{baseline}})}{\text{mean}(\text{BOLD}_{\text{baseline}})} \times 100$$
3. Analysis of explicit smoking behavior of participants
 1. Import the participant responses to questionnaires (i.e., QSU-b, VAS-C, CO measure, and cigarettes per day) to MATLAB.
 2. Test normality of the data using a one-sample Kolmogorov-Smirnov test from MATLAB.
 3. A one-sample t-test should be used to compare responses of different questionnaires for each participant, and a paired sample t-test to compare scores between the experimental and control groups.
4. Analysis of the implicit attitude towards craving-eliciting cues
 1. Extract the reaction time (RT) of affective priming trials for each participant from the log files generated by presentation software.
 2. Remove the outliers based on the RT (i.e., do not include trials with a RT longer than the 2x the standard deviation of the mean RT of the participant).
 3. Test normality of the data using a one-sample Kolmogorov-Smirnov test from MATLAB.
 4. Compare downregulation effects on the median reaction times of unique combinations of primes (craving-inducing and neutral images) and targets (positive and negative words) for each participant, and compare between the experimental and control groups using a paired wise t-test.

Representative Results

Four patients were recruited based on their scores on the Fagerström Test for Nicotine Dependence (FTND)⁴⁵ questionnaire for medium-level nicotine dependence (FTND score >4) and the number of cigarettes smoked every day (>15). In addition, it was ensured that the participants did not have any tattoo or metallic implants as per MRI safety measures of the institution. Five rtfMRI sessions were performed for each participant, in which the first four sessions were conducted over 2 weeks (2 sessions per week), and the fifth session was conducted 6 months after the fourth session. Participants were asked to abstain from smoking at least 3 h before each session.

On day 1, participants underwent pre-training (before the neurofeedback training) sessions in order to obtain baseline implicit behavioral responses to the pictures that elicit craving behavior. On sessions 2 and 3, neurofeedback training (**Figure 2C**) was performed to train downregulation of the BOLD signal in the left (ROI1) and right (ROI2) anterior insular cortices as ROIs. A post-training (after the neurofeedback training; session 4) session that was identical to the pre-training session was then performed. In order to evaluate the long-term effects of neurofeedback training on implicit behavior, a follow-up session similar to the post-training session was conducted 6 months after the post-training session. During the pre-training session (**Figure 2A**), participants were not performing any tasks during the regulation block, and feedback was not provided to them. However, during the post-training and follow-up sessions, participants used self-regulation strategies learned

during the training period. Participants were provided with contingent feedback (monetary reward) at the end of each regulation block. The figures (Figure 4, Figure 5, Figure 6) show sample data from four participants in the experimental group. The data presented is related to participants' neurofeedback performances and changes in craving behaviors, assessed by the questionnaires and affective priming task across the neurofeedback fMRI sessions.

Participants learned to significantly downregulate BOLD signals ($t_{df} = 3.14, p < 0.05$, two-tailed paired sample t-test) in the bilateral insular cortex with neurofeedback training. The success of the participants was estimated by computing the percentage change in the BOLD signal equation as explained below.

$$\text{Reward} = (\text{mean}(\text{BOLD}_{\text{base}} - \text{BOLD}_{\text{reg}})_{\text{roi1}} + (\text{BOLD}_{\text{base}} - \text{BOLD}_{\text{reg}})_{\text{roi2}} - (\text{BOLD}_{\text{base}} - \text{BOLD}_{\text{reg}})_{\text{roi3}}) * 0.1 \text{ Euro}$$

Where: the left anterior insula (ROI1) and right anterior insula (ROI2) were selected based on anatomical landmarks. The primary motor area (M1) was selected as a reference ROI, namely ROI3, to remove the effect of global BOLD increase and BOLD fluctuation due to head movement.

The lower the value of percentage change in the BOLD signal, the higher the success rate of participants in downregulating the bilateral insular cortex (Figure 4). However, the participants did not manage to maintain the learned downregulation during the follow-up session. In addition, we observed a significant overall reduction ($t_{df} = 2.78, p < 0.05$, two-tailed one sample t-test) in the explicit smoking behavior as measured by the CPD (Figure 5A) during the third and the fourth rtfMRI sessions, which further decreases during the follow-up session.

Similarly, we observed a significant reduction in scores for the smoking behavior questionnaires such as the QSU-b (pre-training scores: $t_{df} = 11.1$; post-training scores: $t_{df} = 6.5, p < 0.05$, one sample t-test; Figure 5B) and VAS-C (pre-training scores: $t_{df} = 13.7$; post-training scores: $t_{df} = 16.07, p < 0.05$, two-tailed paired sample t-test; Figure 5C). However, in the case of implicit craving behavior (Figure 6), it was observed that the reaction times (ms) were significantly lower in the tasks presented after the downregulation block compared to the tasks presented after the baseline block. In the affective priming task, there are four combinations of the prime cue (craving eliciting-cue and its neutral counterpart) and target word (positive and negative valence). Out of the abovementioned four combinations, two combinations of priming cue and target cue [i.e., prime: neutral & target: positive ($t_{df} = 2.97$) and prime: craving & target: positive ($t_{df} = 2.78$)] showed significantly ($p < 0.05$) faster reaction times in the task after the downregulation blocks. The overall reduction in reaction time for the tasks after the baseline and regulation blocks may be attributed to the practice effect. However, the reduction in reaction times for the combinations of prime (craving & neutral) and positive target words (Figure 6B) indicates a change in the participant's perceived valence of the craving-inducing cues.

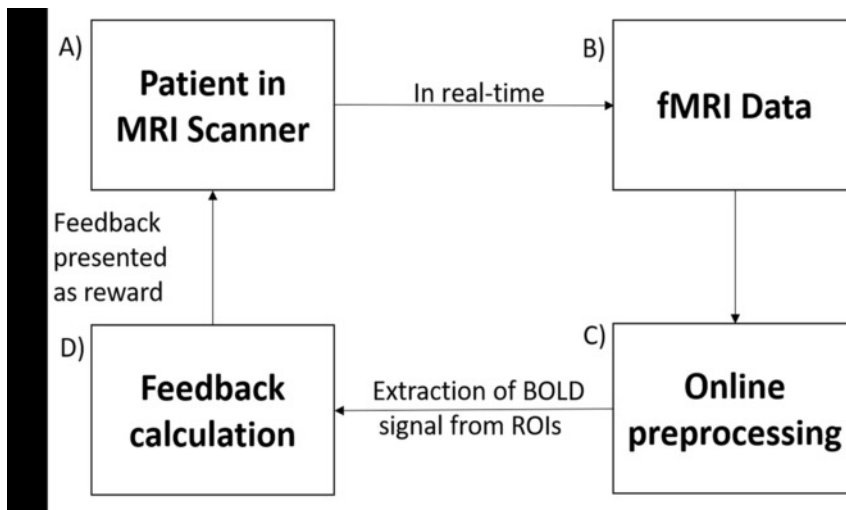


Figure 1: Real-time fMRI set-up. Real-time fMRI-based neurofeedback system is comprised of the following subsystems: (A) participant in the scanner, (B) signal acquisition using an echo planar imaging (EPI) pulse sequence, (C) online preprocessing of the data acquired, (D) computation of the feedback according to the hypothesis, and (E) signal feedback via the scanner projection system. [Please click here to view a larger version of this figure.](#)

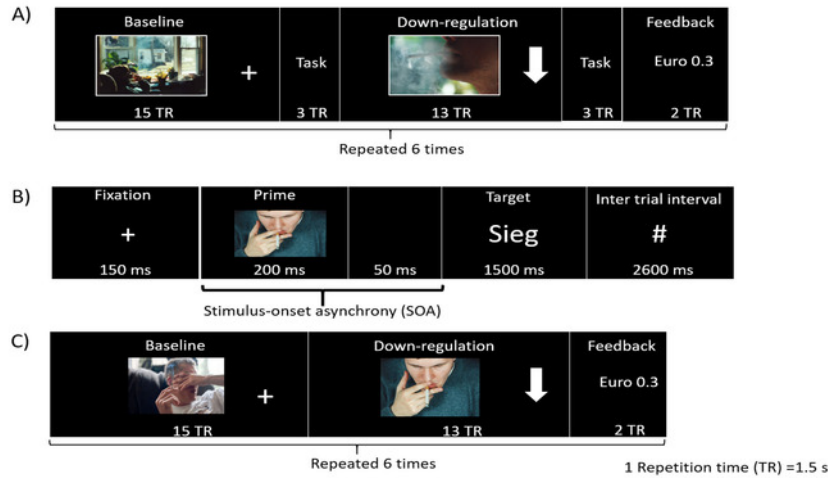


Figure 2: Experimental paradigm. (A) Schematic illustration of the experimental paradigm for pre-training, post-training, and follow-up sessions. The protocol consists of six alternating blocks of baseline and regulation. Each block was followed by an affective priming task. (B) The affective priming task used here evaluates the effect of downregulation on implicit attitude towards craving cues. It consists of a prime (craving eliciting picture or neutral counterpart picture), which is then followed by a target word (positive or negative valence). The word “Sieg” has positive valence, and it is a German word meaning “victory”. (C) Each rfMRI training run consists of baseline, downregulation, and feedback blocks in that order repeated six times. [Please click here to view a larger version of this figure.](#)

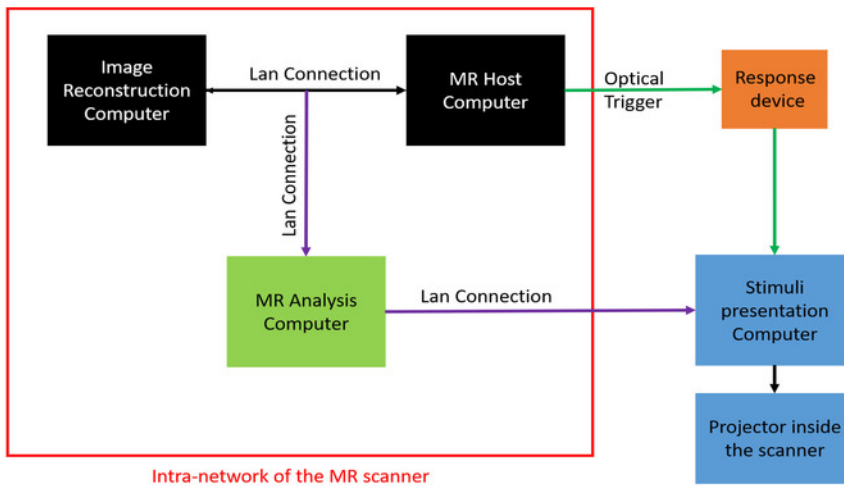


Figure 3: Real-time fMRI hardware set-up. The real-time fMRI set up consists of following three subsystems: (1) image reconstruction and MR host computer (black), (2) real-time MRI analysis computer (green), and (3) stimulus presentation computer and projector (blue). The LAN connections presented in purple color are added to the existing standard fMRI set-up. The optical trigger (dark green) is connected to the stimulus presentation computer through an MR-compatible response device (orange). [Please click here to view a larger version of this figure.](#)

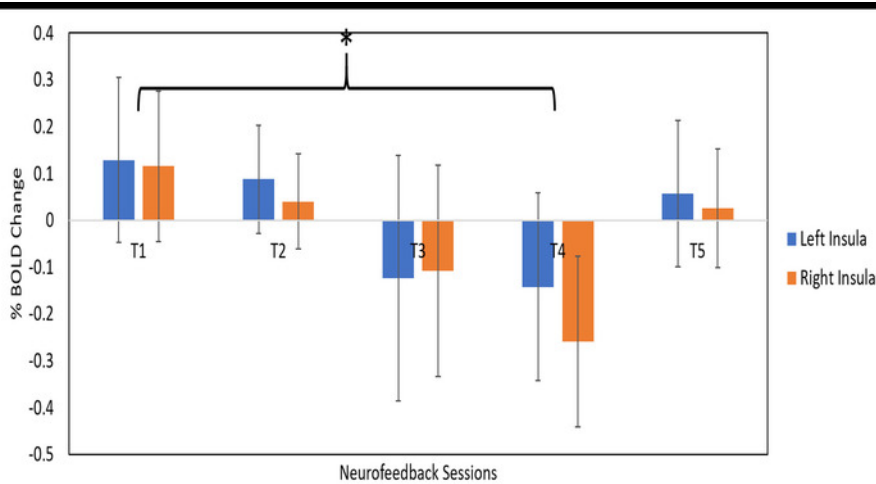


Figure 4: Percentage change in BOLD signal. The figure represents the percentage change in BOLD signal in the left (blue) and right (orange) insular cortices during the pre-training (T1), neurofeedback training (T2, T3), post-training (T4), and follow-up (6 months after post-training session; T5). The participant showed a significant (paired sample t-test; $*p < 0.05$) reduction in BOLD activity during the downregulation block compared to the baseline block (mentioned above). A negative value of percentage change in BOLD signal represents downregulation. Error bars represent the standard deviation in the percentage change values of downregulation trials. [Please click here to view a larger version of this figure.](#)

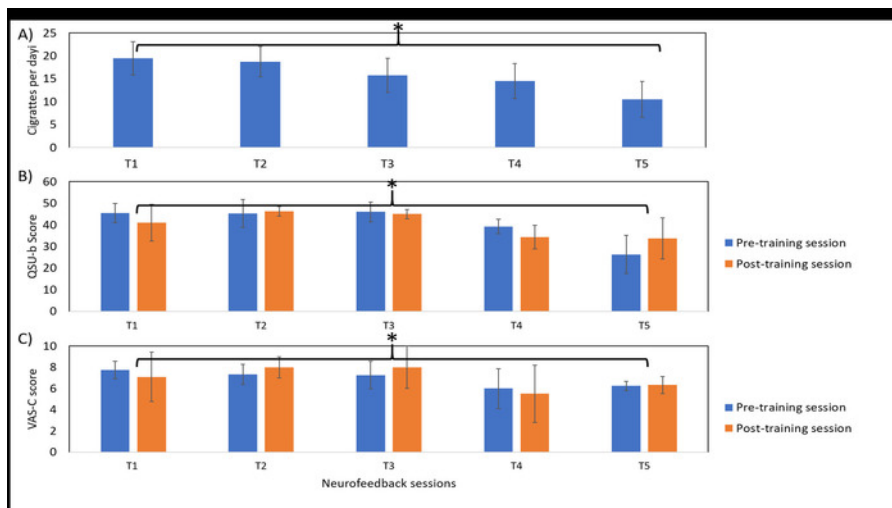


Figure 5: Explicit craving behavior. The figure represents explicit craving behavior of the participant, namely Visual Analog Scale for Craving (VAS-C), Questionnaire of Smoking Urges-Brief (QSU-b) and number of cigarettes per day (CPD) during the during the pre-training (T1), neurofeedback training (T2, T3), post-training (T5), and follow-up (6 months after post-training session; T5). Higher scores indicate higher craving levels. These results show that there is a significant (one sample t-test; $*p < 0.05$) overall reduction in scores of all the scales, indicating a reduction in explicit craving behavioral of the participant. [Please click here to view a larger version of this figure.](#)

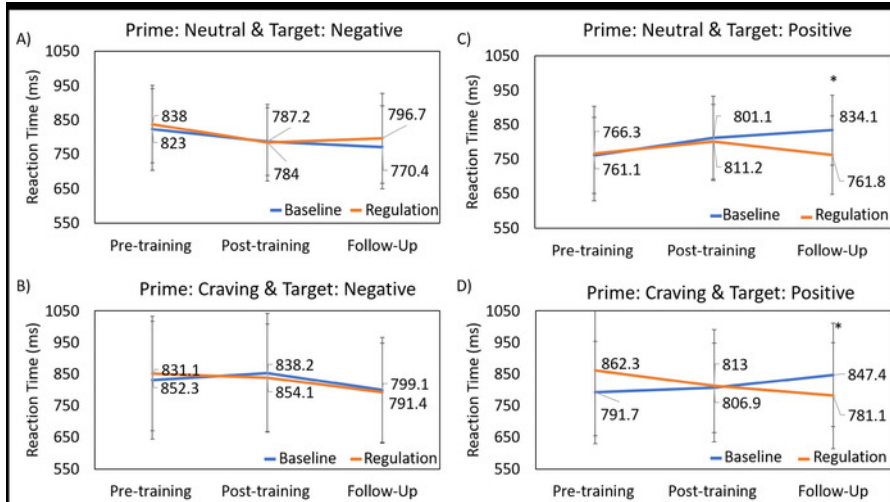


Figure 6: Implicit craving behavior. The figure represents implicit behavior of the participant towards the craving-eliciting picture cues and its counterpart neutral pictures, assessed by an affective priming task across fMRI sessions (pre-training, post-training, and follow-up). The reaction time (ms) is presented for the baseline (blue) and downregulation (orange) blocks. Reaction times (ms) between the baseline and regulation blocks for a neutral (C) and craving (D)-inducing prime picture were significantly different (paired sample t-test; * $p < 0.05$) in the follow-up session. [Please click here to view a larger version of this figure.](#)

Pre-training Session (T1)	Neurofeedback training (T2 & T3)	Post- neurofeedback training (T4)	Follow-up (6 months) session (T5)
Smoking questionnaires	Smoking questionnaires	Smoking questionnaires	Smoking questionnaires
8 fMRI session and with priming task	4 fMRI -based neurofeedback training session	8 fMRI session and with priming task	8 fMRI session and with priming task
Anatomical Scan	1 transfer neurofeedback run	Anatomical Scan	Anatomical Scan
Resting state fMRI	Anatomical Scan	Resting state fMRI	Resting state fMRI
Diffusion Tensor Imaging (DTI)		Diffusion Tensor Imaging (DTI)	Diffusion Tensor Imaging (DTI)

Table 1: Experimental paradigm for the five sessions consisting of questionnaires and real-time fMRI training sessions.

Discussion

Results from four participants demonstrate the possibility for cigarette smokers to learn to downregulate activation in the bilateral anterior insula in the presence of a craving-eliciting cues. Changes in the implicit and explicit smoking behaviors after neurofeedback training in the sample participant may be related to learned downregulation, as the participant did not go through any other clinical or experimental interventions during the course of the experiment. Change in the participant’s implicit behavior may indicate a change in the attentional bias towards the craving eliciting pictures. The changes in reaction time for positive target words indicate that the participant’s attentional bias may have shifted towards the neutral valence cues after downregulation training. This may indicate the possibility that participants were less affected by the craving-inducing images after downregulation of the insula than during the baseline condition, indicating potential reduction of craving due to downregulation.

This result is in line with the explicit behavior scores, as participants reported less craving and a reduced average number of cigarettes per day (to 10 per day) after 6 months into the study, compared to 20 per day before enrollment. This result is particularly notable because no clinical or experimental interventions were involved during the 6 month period between the post-training and follow-up sessions. While the above reduction in craving and number of cigarettes smoked per day cannot be related with certainty to the neurofeedback training alone, these results have encouraging implications in treating relapses. We are mindful of the need for a larger sample size and more robust statistics for a more reliable conclusion.

Several neuroimaging studies have demonstrated a role of the insula in urges for drugs like alcohol^{46,47}, cocaine^{15,48}, and heroin⁴⁹. Another application of the current protocol may be in obese patients. It is known that anterior and mid-dorsal insula become highly activated when hungry obese patients are presented with images of high caloric food compared to lean subjects⁵⁰. The current protocol may be generalized to other addictions as a therapeutic intervention by using different drug-associated cues.

These preliminary results suggest that with further progress in this approach, fMRI-based neurofeedback may lead to therapeutic intervention, in line with observations made in other studies^{51,52,53,54}. Neurofeedback as a clinical intervention is still in an early stage; although, many randomized clinical trials (RCTs) have been conducted in patients with certain clinical conditions such as attention deficit hyperactivity disorder (ADHD). In the ADHD clinical trials, patients were trained to lower the amplitude in low-frequency EEG oscillations (e.g., delta and theta EEG bands), which are known to be high in patients with ADHD. These RCTs demonstrated that patients learned to lower amplitudes using neurofeedback training with improvement in ADHD symptoms^{55,56,57,58}.

In addition, the clinical effect-size due to neurofeedback training may be higher than traditional computerized attention training. Similarly, RCTs have validated improvement in motor functions of stroke patients by combining EEG-based neurofeedback training with existing therapeutic approaches⁵⁹ (physiotherapy) or modern stimulation approaches [e.g., functional electric stimulator⁶⁰ (FES), *transcranial magnetic stimulation*⁶¹ (TMS), and robotic assistive therapy^{62,63}]. However, the observed improvements in motor function have also been observed as highly inconsistent in different patients, possibly due to variability in the locations and sizes of the brain lesions⁶⁴.

Although several fMRI-based neurofeedback studies have demonstrated behavioral improvements in a psychiatric and neurological disorders, no RCTs have been conducted so far using this approach. Despite its benefits, rfMRI-based neurofeedback presents certain hindrances for its use in a clinical setting, including high running costs and a claustrophobic, noisy environment inside the scanner. These limitations also apply to the current protocol. Therefore, it is important to identify an approach that can be used to supplement rfMRI with a cheaper modality like EEG- or fNIRS-based neurofeedback approaches. Thus, in future studies, a protocol could be developed that combines both fMRI-based neurofeedback and EEG- or fNIRS-based neurofeedback training approaches.

In the initial stage of the protocol, patients would be trained to downregulate the insular cortex using fMRI-based neurofeedback training, and simultaneous EEG recording will be conducted to assess neuroelectric components that correlate with learned downregulation of the insular cortex. Later, a model of activation patterns of deep brain structures (e.g., insula) from surface EEG data could be developed. This can be achieved by using existing methods of source localization algorithms⁶⁵ that allow for construction of a 3D model of electrical activity in the brain, based on exact low resolution electromagnetic tomography (eLORETA)⁶⁶ or the EEG fingerprint method⁶⁷. In the second stage of the proposed protocol, patients could be given an extended neurofeedback training with an EEG-based neurofeedback approach. Thus, this protocol provides a possibility to train (neurofeedback training) patients for longer periods of time in a user-friendly environment and at a lower cost. In this way, this may allow for the translation of scientifically rigorous findings from rfMRI neurofeedback training to a portable and affordable clinical system for the treatment of psychiatric and neurological disorders. The further use of this noninvasive method for recording both neuronal activity and hemodynamic activity in the brain during neurofeedback experiments raises exciting new possibilities for clinical treatment and rehabilitation.

Disclosures

The authors have nothing to disclose.

Acknowledgments

This study was supported by Comisión Nacional de Investigación Científica y Tecnológica de Chile (Conicyt) through Fondo Nacional de Desarrollo Científico y Tecnológico, Fondecyt Postdoctoral grant (no. 3100648) Fondecyt Regular (projects no. 1171313 and no. 117132) and CONICYT PIA/Anillo de Investigación en Ciencia y Tecnología ACT172121.

References

1. Fernandez, T. *et al.* EEG and behavioral changes following neurofeedback treatment in learning disabled children. *Clinical Electroencephalography*. **34**, 145-152 (2003).
2. Scarapicchia, V., Brown, C., Mayo, C., Gawryluk, J. R. Functional Magnetic Resonance Imaging and Functional Near-Infrared Spectroscopy: Insights from Combined Recording Studies. *Frontiers in Human Neuroscience*. **11**, 419 (2017).
3. Hinault, T., Larcher, K., Zazubovits, N., Gotman, J., Dagher, A. Spatio-temporal patterns of cognitive control revealed with simultaneous electroencephalography and functional magnetic resonance imaging. *Human Brain Mapping*. (2018).
4. Grech, R. *et al.* Review on solving the inverse problem in EEG source analysis. *Journal of NeuroEngineering and Rehabilitation*. **5**, 25 (2008).
5. Van Essen, D. C. *et al.* The Human Connectome Project: a data acquisition perspective. *NeuroImage*. **62**, 2222-2231 (2012).
6. World Health Organization. *WHO Report on the Global Tobacco Epidemic, 2017*. Geneva: World Health Organization (2017).
7. Ringlever, L., Otten, R., de Leeuw, R. N., Engels, R. C. Effects of parents' education and occupation on adolescent smoking and the mediating role of smoking-specific parenting and parent smoking. *European Addiction Research*. **17**, 55-63 (2011).
8. Malaiyandi, V., Sellers, E. M., Tyndale, R. F. Implications of CYP2A6 genetic variation for smoking behaviors and nicotine dependence. *Clinical Pharmacology and Therapeutics*. **77**, 145-158 (2005).
9. Brody, A. L. *et al.* Neural substrates of resisting craving during cigarette cue exposure. *Biological Psychiatry*. **62**, 642-651 (2007).
10. Childress, A. R. *et al.* Cue reactivity and cue reactivity interventions in drug dependence. *NIDA Research Monograph*. **137**, 73-95 (1993).
11. Claus, E. D., Kiehl, K. A., Hutchison, K. E. Neural and behavioral mechanisms of impulsive choice in alcohol use disorder. *Alcoholism, Clinical and Experimental Research*. **35**, 1209-1219 (2011).
12. Franklin, T. R. *et al.* Limbic activation to cigarette smoking cues independent of nicotine withdrawal: a perfusion fMRI study. *Neuropsychopharmacology*. **32**, 2301-2309 (2007).
13. Grusser, S. M. *et al.* Cue-induced activation of the striatum and medial prefrontal cortex is associated with subsequent relapse in abstinent alcoholics. *Psychopharmacology*. **175**, 296-302 (2004).
14. Buhler, M. *et al.* Nicotine dependence is characterized by disordered reward processing in a network driving motivation. *Biological Psychiatry*. **67**, 745-752 (2010).
15. Bonson, K. R. *et al.* Neural systems and cue-induced cocaine craving. *Neuropsychopharmacology*. **26**, 376-386 (2002).
16. Brody, A. L. *et al.* Brain metabolic changes during cigarette craving. *Archives of General Psychiatry*. **59**, 1162-1172 (2002).
17. Contreras, M., Ceric, F., Torrealba, F. Inactivation of the interoceptive insula disrupts drug craving and malaise induced by lithium. *Science*. **318**, 655-658 (2007).
18. Naqvi, N. H., Rudrauf, D., Damasio, H., Bechara, A. Damage to the insula disrupts addiction to cigarette smoking. *Science*. **315**, 531-534 (2007).
19. Hollander, J. A., Lu, Q., Cameron, M. D., Kamenecka, T. M., Kenny, P. J. Insular hypocretin transmission regulates nicotine reward. *Proceedings of the National Academy of Sciences of the United States of America*. **105**, 19480-19485 (2008).

20. Forget, B., Pushparaj, A., Le Foll, B. Granular insular cortex inactivation as a novel therapeutic strategy for nicotine addiction. *Biological Psychiatry*. **68**, 265-271 (2010).
21. Scott, D., Hiroi, N. Deconstructing craving: dissociable cortical control of cue reactivity in nicotine addiction. *Biological Psychiatry*. **69**, 1052-1059 (2011).
22. Buczkowski, K., Marcinowicz, L., Czachowski, S., Piszczek, E. Motivations toward smoking cessation, reasons for relapse, and modes of quitting: results from a qualitative study among former and current smokers. *Patient Prefer Adherence*. **8**, 1353-1363 (2014).
23. Hughes, J. R., Stead, L. F., Hartmann-Boyce, J., Cahill, K., Lancaster, T. Antidepressants for smoking cessation. *Cochrane Database of Systematic Reviews*. CD000031 (2014).
24. Bedi, G. *et al.* Incubation of cue-induced cigarette craving during abstinence in human smokers. *Biological Psychiatry*. **69**, 708-711 (2011).
25. Bassett, J. F., Dabbs, J. M., Jr. A portable version of the go/no-go association task (GNAT). *Behavior Research Methods*. **37**, 506-512 (2005).
26. Huijding, J., de Jong, P. J., Wiers, R. W., Verkooijen, K. Implicit and explicit attitudes toward smoking in a smoking and a nonsmoking setting. *Addictive Behaviors*. **30**, 949-961 (2005).
27. Sherman, S. J., Rose, J. S., Koch, K., Presson, C. C., Chassin, L. Implicit and explicit attitudes towards cigarette smoking: The effect of context and motivation. *Journal of Social and Clinical Psychology*. **22**, 13-39 (2003).
28. Swanson, J. E., Rudman, L. A., Greenwald, A. G. Using the Implicit Association Test to investigate attitude-behavior consistency for stigmatized behavior. *Cognition and Emotion*. **15**, 207-230 (2001).
29. Asgaard, G. L., Gilbert, D. G., Malpass, D., Sugai, C., Dillon, A. Nicotine primes attention to competing affective stimuli in the context of salient alternatives. *Experimental and Clinical Psychopharmacology*. **18**, 51-60 (2010).
30. Gilbert, D. G. *et al.* Effects of nicotine on brain responses to emotional pictures. *Nicotine & Tobacco Research*. **6**, 985-996 (2004).
31. Czyzewska, M., Graham, R. Implicit and explicit attitudes to high- and low-calorie food in females with different BMI status. *Eating Behaviors*. **9**, 303-312 (2008).
32. Gilbert, D.G., Rabinovich, N.E. *International smoking images series (with neutral counterparts)*. Southern Illinois University: Integrative Neuroscience Laboratory, Department of Psychology. (1999).
33. Bandettini, P. A., Wong, E. C., Hinks, R. S., Tikofsky, R. S., Hyde, J. S. Time course EPI of human brain function during task activation. *Magnetic Resonance Medicine*. **25**, 390-397 (1992).
34. Goebel, R. BrainVoyager - past, present, future. *NeuroImage*. **62**, 748-756 (2012).
35. Poline, J. B., Worsley, K. J., Holmes, A. P., Frackowiak, R. S., Friston, K. J. Estimating smoothness in statistical parametric maps: variability of p values. *Journal of Computer Assisted Tomography*. **19**, 788-796 (1995).
36. Johnson, K. A. *et al.* Intermittent "real-time" fMRI feedback is superior to continuous presentation for a motor imagery task: a pilot study. *Journal of Neuroimaging*. **22**, 58-66 (2012).
37. Yoo, S. S., Jolesz, F. A. Functional MRI for neurofeedback: feasibility study on a hand motor task. *Neuroreport*. **13**, 1377-1381 (2002).
38. Craig, A. D. How do you feel--now? The anterior insula and human awareness. *Nature reviews Neuroscience*. **10**, 59-70 (2009).
39. Cox, L. S., Tiffany, S. T., Christen, A. G. Evaluation of the brief questionnaire of smoking urges (QSU-brief) in laboratory and clinical settings. *Nicotine & Tobacco Research*. **3**, 7-16 (2001).
40. Wewers, M. E., Rachfal, C., & Ahijevych, K. A psychometric evaluation of a visual analogue scale of craving for cigarettes. *Western Journal of Nursing Research*. **12**, 672-681 (1990).
41. Allen, D. R., Browse, N. L., Rutt, D. L., Butler, L., Fletcher, C. The effect of cigarette smoke, nicotine, and carbon monoxide on the permeability of the arterial wall. *Journal of Vascular Surgery*. **7**, 139-152 (1988).
42. Weiskopf, N. *et al.* Real-time functional magnetic resonance imaging: methods and applications. *Magnetic Resonance Imaging*. **25**, 989-1003 (2007).
43. Sladky, R. *et al.* Slice-timing effects and their correction in functional MRI. *NeuroImage*. **58**, 588-594 (2011).
44. Mazziotta, J. *et al.* A probabilistic atlas and reference system for the human brain: International Consortium for Brain Mapping (ICBM). *Philosophical Transactions of the Royal Society of London: Series B, Biological Sciences*. **356**, 1293-1322 (2001).
45. Heatherton, T. F., Kozlowski, L. T., Frecker, R. C., Fagerstrom, K. O. The Fagerstrom Test for Nicotine Dependence: a revision of the Fagerstrom Tolerance Questionnaire. *British Journal of Addiction*. **86**, 1119-1127 (1991).
46. Myrick, H. *et al.* Differential brain activity in alcoholics and social drinkers to alcohol cues: relationship to craving. *Neuropsychopharmacology*. **29**, 393-402 (2004).
47. Tapert, S. F., Brown, G. G., Baratta, M. V., Brown, S. A. fMRI BOLD response to alcohol stimuli in alcohol dependent young women. *Addictive Behaviors*. **29**, 33-50 (2004).
48. Kilts, C. D., Gross, R. E., Ely, T. D., Drexler, K. P. The neural correlates of cue-induced craving in cocaine-dependent women. *American Journal of Psychiatry*. **161**, 233-241 (2004).
49. Li, Q. *et al.* Assessing cue-induced brain response as a function of abstinence duration in heroin-dependent individuals: an event-related fMRI study. *PLoS One*. **8**, e62911 (2013).
50. Frank, S., Kullmann, S., Veit, R. Food related processes in the insular cortex. *Front Hum Neurosci*. **7**, 499 (2013).
51. deCharms, R. C. *et al.* Control over brain activation and pain learned by using real-time functional MRI. *Proceedings of the National Academy of Sciences of the United States of America*. **102**, 18626-18631 (2005).
52. Ruiz, S., Birbaumer, N., Sitaram, R. Abnormal Neural Connectivity in Schizophrenia and fMRI-Brain-Computer Interface as a Potential Therapeutic Approach. *Frontiers in Psychiatry*. **4**, 17 (2013).
53. Habes, I. *et al.* Pattern classification of valence in depression. *NeuroImage Clinical*. **2**, 675-683 (2013).
54. Li, X. *et al.* Volitional reduction of anterior cingulate cortex activity produces decreased cue craving in smoking cessation: a preliminary real-time fMRI study. *Addiction Biology*. **18**, 739-748 (2013).
55. Lubar, J. F., Swartwood, M. O., Swartwood, J. N., O'Donnell, P. H. Evaluation of the effectiveness of EEG neurofeedback training for ADHD in a clinical setting as measured by changes in T.O.V.A. scores, behavioral ratings, and WISC-R performance. *Biofeedback and Self-Regulation*. **20**, 83-99 (1995).
56. Janssen, T. W. *et al.* A randomized controlled trial into the effects of neurofeedback, methylphenidate, and physical activity on EEG power spectra in children with ADHD. *Journal of Child Psychology and Psychiatry*. **57**, 633-644 (2016).
57. Mayer, K., Wyckoff, S. N., Fallgatter, A. J., Ehlis, A. C., Strehl, U. Neurofeedback as a nonpharmacological treatment for adults with attention-deficit/hyperactivity disorder (ADHD): study protocol for a randomized controlled trial. *Trials*. **16**, 174 (2015).
58. Gevensleben, H. *et al.* Distinct EEG effects related to neurofeedback training in children with ADHD: a randomized controlled trial. *International Journal of Psychophysiology*. **74**, 149-157 (2009).

59. Ramos-Murguialday, A. *et al.* Brain-machine interface in chronic stroke rehabilitation: a controlled study. *Annals of Neurology*. **74**, 100-108 (2013).
60. Biasucci, A. *et al.* Brain-actuated functional electrical stimulation elicits lasting arm motor recovery after stroke. *Nature Communication*. **9**, 2421 (2018).
61. Du, J. *et al.* Effects of repetitive transcranial magnetic stimulation on motor recovery and motor cortex excitability in patients with stroke: a randomized controlled trial. *European Journal of Neurology*. **23**, 1666-1672 (2016).
62. Ang, K. K. *et al.* Facilitating effects of transcranial direct current stimulation on motor imagery brain-computer interface with robotic feedback for stroke rehabilitation. *Archives of Physical Medicine and Rehabilitation*. **96**, S79-87 (2015).
63. Wolbrecht, E. T., Chan, V., Reinkensmeyer, D. J., Bobrow, J. E. Optimizing compliant, model-based robotic assistance to promote neurorehabilitation. *IEEE Transactions on Neural Systems and Rehabilitation Engineering*. **16**, 286-297 (2008).
64. Sitaram, R. *et al.* Closed-loop brain training: the science of neurofeedback. *Nature Reviews Neuroscience*. **18**, 86-100 (2017).
65. Simkin, D. R., Thatcher, R. W., Lubar, J. Quantitative EEG and neurofeedback in children and adolescents: anxiety disorders, depressive disorders, comorbid addiction and attention-deficit/hyperactivity disorder, and brain injury. *Child and Adolescent Psychiatric Clinics of North America*. **23**, 427-464 (2014).
66. Pascual-Marqui, R. D. *et al.* Assessing interactions in the brain with exact low-resolution electromagnetic tomography. *Philosophical transactions: Series A, Mathematical, physical, and engineering sciences*. **369**, 3768-3784 (2011).
67. Meir-Hasson, Y., Kinreich, S., Podlipsky, I., Hendler, T., Intrator, N. An EEG Finger-Print of fMRI deep regional activation. *NeuroImage*. **102 Pt 1**, 128-141 (2014).